Analysis of Internal Temperature Variations of Lithium-Ion Batteries During Fast Charging

1st Nessa Fereshteh Saniee
WMG
University of Warwick
Coventry, United Kingdom
n.fereshteh-saniee@warwick.ac.uk

2nd Nithin Somasundaran
WMG
University of Warwick
Coventry, United Kingdom
nithin.somasundaran@warwick.ac.uk

3rd Begum Gulsoy
WMG
University of Warwick
Coventry, United Kingdom
begum.gulsoy.1@warwick.ac.uk

4th Tim Vincent
WMG
University of Warwick
Coventry, United Kingdom
t.a.vincent@warwick.ac.uk

5th Mark Amor-segan
WMG
University of Warwick
Coventry, United Kingdom
mark.amor-segan@warwick.ac.uk

6th James Marco
WMG
University of Warwick
Coventry, United Kingdom
james.marco@warwick.ac.uk

***Abstract*—One of the major challenges that limits the fast charging of Lithium-ion batteries is Lithium (Li) plating at low temperatures. To reduce Li-plating an increased environmental temperature is commonly used. However, the uncertainties in the measurement of key battery internal states such as temperature, is a limiting factor to find the best fast charging profile that considers battery performance, degradation, and safety of the electric vehicles (EVs). We have used our state-of-the-art instrumented cells equipped with internal data acquisition and microcontroller, forming smart cells, that enable sensor data to be transmitted via a USB to a data logger. We demonstrate here that commercially available 21700 format cells were successfully instrumented and gave direct information on internal temperature for continuous fast charging rates from C/2 to 2.5C. The internal temperature was found to be considerably higher than that of the surface of the cell (between 10 and 14°C at 2.5C charge rate). A gradient of up to 2°C was found between the positive and negative end of each cell that became more prominent for higher charge rates. Li-plating was detected for all C-rates below 25°C even though, the internal temperature rose above 30°C when the cells were charged at 2.5C with an ambient temperature of 0°C. At a higher ambient temperature of 40°C, the cell's internal temperature rose (to ~62°C) beyond the safe limits defined by the manufacturer's datasheet whilst the external temperature recorded (~52°C) was within the manufacturer's defined safe operating limits.**

Keywords—Fast charging, Li-ion battery experimentation, Cell instrumentation, Cell temperature sensing, Li-Plating

I. INTRODUCTION

Decarbonisation of the transport system is a key principle on the agenda of many developed countries for the next 2 decades. Hence the demand for fast charging of Li-ion batteries (LIB) has increased rapidly for high-energy-density cells. To reduce the range anxiety of the consumers towards electrification, the US advanced battery consortium (USABC) has called for a goal of fast charging to 80% state of charge (SoC) under 15 minutes [1]. However, whilst trying to achieve this goal, we face uncertainties in the measurement of fundamental internal battery states such as temperature. This uncertainty in temperature measurement increases safety concerns when charging high energy density LIB, using high charge rates as they often have thick electrodes that result in excess heat generated during fast charging [2]. Currently, all the battery testing to optimise the fast charge profile and develop the required time for each C-rate is done using traditional surface-mount sensing such as external thermocouples. The conventional sensing methods face three main challenges: the method of attachment can vary significantly which also has a notable effect on the reported state, the position of the sensor will impact the data recorded (i.e. near the positive or negative electrode), and lack of robust method to monitor the cells internal parameters [3]. The uncertainty of measuring the temperature during fast charging undermines the safety regulation and does not allow a better understanding of the degradation modes associated with fast charging. This in turn adds further complexity to the thermal management when scaling up battery components into more sophisticated system for EVs and future electric aircrafts. Apart from the added safety concerns, the increased internal temperature will lead to fading capacity and degradation [4]. But this is not the only degradation mechanism that occurs when fast charging LIB. Li-plating formed on the surface of the graphite-based anode has separate issues when it forms a dendrite that can lead to capacity fade, short-circuiting, and electrolyte consumption [5]. To monitor the Li-plating whilst varying the temperature, a method called voltage relaxation profile (VRP) has been used [6,7]. VRP relies on detecting the reversible portion of the Li metal that was plated on the negative electrode during charging. The intercalation of the plated Li- ion on the anode causes a distinct voltage plateau of the cell voltage when measuring the open circuit voltage (OCV) [6]. The amount of plating is directly attributed to the amount of Li stripping during the relaxation immediately after charging. The $\partial v/\partial t$ during rest phase after charge [7] can reveal the end of Li stripping that believed to be proportional to the amount of reversible Li plated on the anode. The increased period of stripping indicates that a greater amount of plating occurred during the fast charge. Considering the effect of temperature on cell degradation at both low and high temperature range, it is important to precisely monitor the cell temperature across the length of the cell and more importantly the core temperature of the cylindrical test when fast charging. This will allow the optimum fast charging profile to be found, staying within the safe temperatures, whilst monitoring the Li-plating. To reduce safety concerns around fast charging of LIB, there is a need to understand, detect, and characterise the effect of fast charging on internal temperature accurately and precisely. The following sections address these issues.

II. EXPERIMENTAL PROCEDURE

A. Cell cycling and tempertaure measurement

Commercially available INR21700 48X Samsung cells with a rated capacity of C=4.8Ah, graphite anode and NMC cathode were selected. A single range (±12.5 A) Maccor cycler was

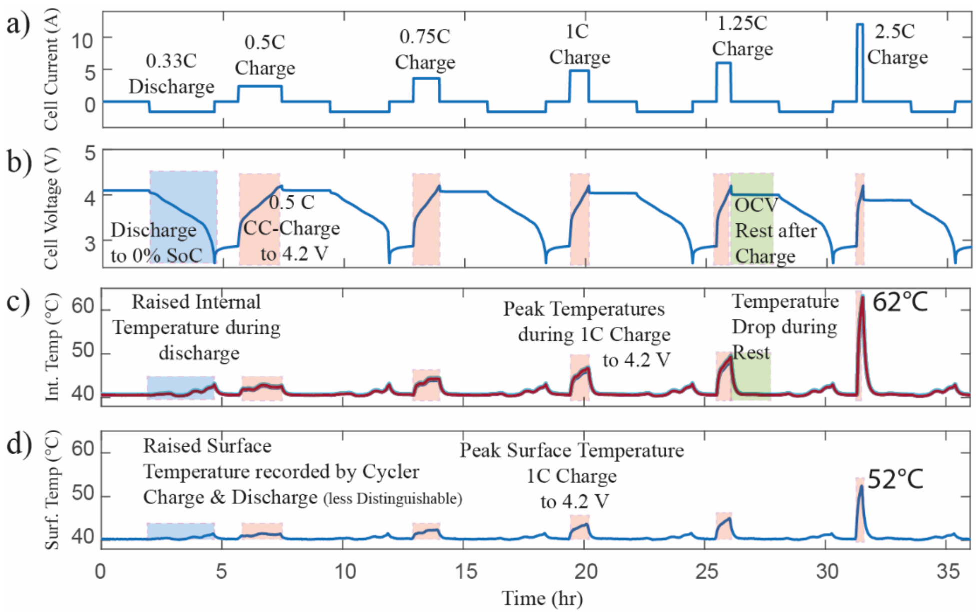

Figure 1 a) Cell Current, b) Cell Voltage c) Cell Temperature measured by Internal Thermistors and d) Surface Temperature measured by the Maccor cycler's external T-type thermocouple during a multiple C-rate Fast Charge program at 40°C. Maximum temperatures are Ext. 52°C and Int. 62°C.

used to charge and also run a Reference Performance Test (RPT) to monitor the quality of the cells and detect the onset of degradation. To measure the total capacity of the cell, they were discharge to 2.5V at 1C (C=4.8 Ah) then at C/10 to measure the residual capacity. To study the effect of temperature on Li-plating during fast-charging, cells were soaked for 2 hours prior testing at temperatures of 0, 5, 10, 25 and 40°C to cover both high and low temperature zones. A Binder environmental chamber was used to change the test temperature. Cells were charged using a constant current (CC) approach to the upper voltage limits of 4.2 V. Fig. 1 pictures a multi-C-rate cycle that was used for each temperature at 0.5, 0.75, 1, 1.25, and 2.5C. Cells were discharged (by 0.33C) between each cycle until a cut-off voltage of 2.5 V was reached. A rest period of two hour was allowed after each charge cycle.

The surface temperature of the centre of each cell was monitored with a T-type thermocouple that was connected to the Maccor cycler and an external K-type thermocouple using a Pico logger. All thermocouples were calibrated prior to testing using a Dry Well calibrator temperature source and referencing the temperature against a Platinum Resistance Thermometer (PRT). The thermocouples and PRT were monitored with a precision thermometer. The equipment used has a traceable calibration to National Standards.

B. Cell instrumentation

Cell instrumentation was performed using the methods reported in [3, 8]. Fig. 2 shows the schematic and micro-computer tomography (CT) pictures of two instrumentation types: Thermistor arrays (-a and -b) and internal single K-type thermocouple (-d and -e). One thermistor array was inserted internally and one mounted on the surface externally with 7 thermistors positioned to give a spatial resolution of 10 mm along the axial length of the cell. Three cells were instrumented using the thermistors and compared with three pristine cells to ensure that the instrumentation did not have detrimental impact on the cells. One cell was instrumented with an internal K-type thermocouple. All cells had two external thermocouples mounted centrally K and T-type (Fig. 2-a and -d). RPT was performed regularly after each step of the instrumentation. The results of the full capacity are shown along with the internal resistance at 100% SoC for 30s 2C discharge pulse.

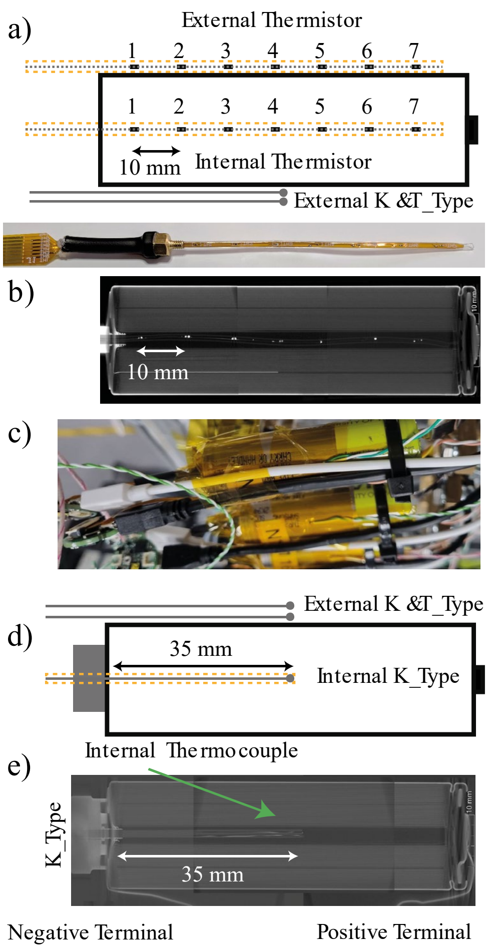

Figure 2 a) Schematic and b) micro-CT images of a 21700 LIB instrumented cells with an array of thermistors. An external array of 7 thermistors also placed externally. c) The setup shows 2 external thermocouples mounted centrally using Kapton tape. The thermistors are 10 mm apart. d) Schematic and e) micro-CT image an instrumented cells with a K-type thermocouple.

TABLE 1: a) CAPACITY AND b) INTERNAL RESISTANCE OF SMART (INSTRUMENTED) AND PRISTINE (AS RECEIVED) CELLS THROUGHOUT THE c) LEGEND FOR RPT TEST DURING THE INSTRUMENTATION PROCESS AND FAST CHARGING (FC) TESTS. STD IS STANDARD DEVIATION.

a)

Cell Type	**Capacity: 1C + 10C (Ah)**				
	1st	**2nd**	**3rd**	**4th**	**5th**
Smart	4.75	4.73	4.66	4.53	4.40
STD	0.01	0.01	0.02	0.04	0.05
Pristine	4.75		4.70	4.60	4.56
STD	0.01		0.02	0.02	0.01

b)

Cell Type	**Resistance @ 100% SoC, 30s pulse (mΩ)**				
Smart	30.21	30.46	31.35	32.37	34.8
STD	0.24	1.60	1.47	2.03	2.83
Pristine	29.08		29.17	29.59	30.1
STD	0.17		0.31	0.20	0.12

c) RPT	**Cell Condition before the RPT**
1st	Pristine
2nd	Instrumented (Smart)
3rd	After fast charge cycle @ 25 and 40°C
4th	After fast charge cycle @ 10 and 5°C
5th	After fast charge cycle @ 0°C

This method was used throughout the fast-charging experiment to ensure that safe operation of the cells.

The results for first to sixth RPT can be seen in Table 1. The instrumentation process did not impact the cell capacity and internal resistance. The average capacity showed a negligible drop of 0.4%. The capacity fades more after the lower temperature cycles that can be attributed to the Li-plating and will be explained in the next section.

III. RESUTS AND DISCUSSION

All cells (instrumented and pristine) were charged with charge rates of 0.5C, 0.75C, 1C, 1.25C and 2.5C continuous charge until voltage reached 4.2V. Fig. 3 highlights the effect of temperature and C-rate on the final capacity in ampere per hour. Lower temperatures and higher C-rates result in the cells reaching the cut off voltage sooner. The highest SoC achieved using the constant current (CC) method was for 40°C temperature at 0.5C charge rate that was 93%. The lowest SoC was 49% at 2.5C and 0°C. In contrast, cells were charged to above 80% SoC at higher temperature range C-rates below 1C (81 and 85% at 25 and 40°C, respectively for 0.75C). The constant voltage (CV) part of the charge to reach 100% state SoC was not considered in this study since some of the Li-plating can be reversed during the CV phase [9]. The maximum temperature observed during charge followed by the rest period was extracted from all four types of temperature measurement devices and compared in Fig. 4 and Fig. 5. The delta rises in temperature observed between the internal and surface thermistors are similar to that of the corresponding K-type thermocouples (± 1°C). This demonstrates that the internal thermistors and K-type thermocouples are both reporting the temperatures

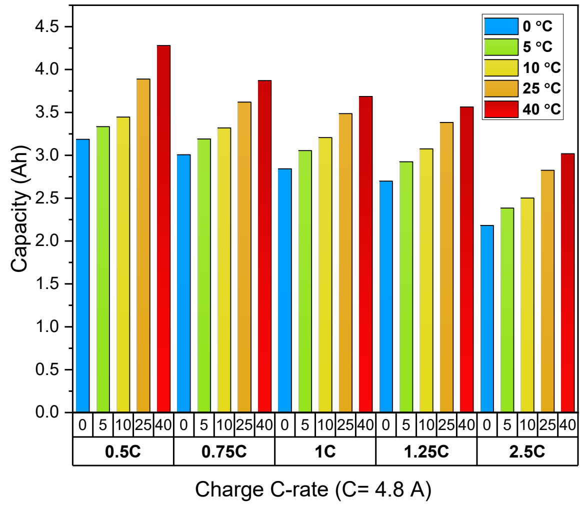

Figure 3 Capacity reached at the end of CC phase when voltage reached upper cut off of 4.2 V for 0.5C, 0.75C, 1C, 1.25C, and 2.5C charge rates and temperatures of 0, 5, 10, 25, and 40°C.

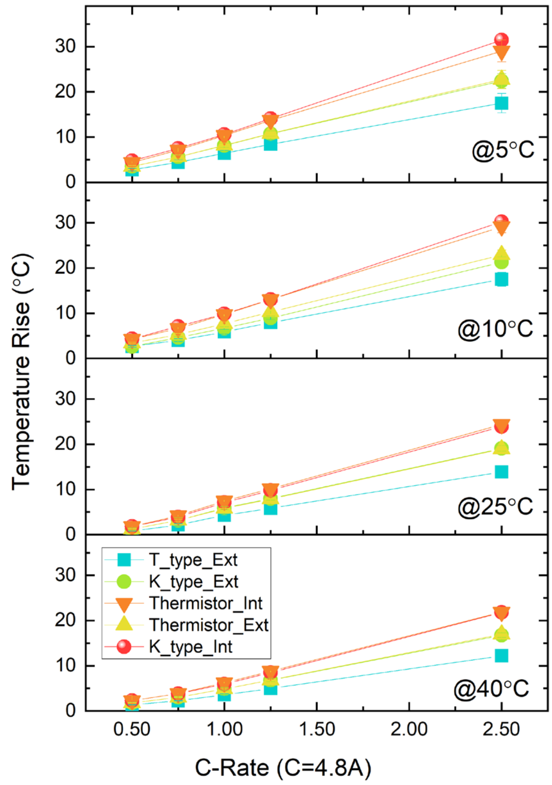

Figure 4 Gradient of maximum temperature rise during the charge and rest period after the charge. Internal- External Temperatures during the CC phase and the relaxation period.

accurately. However, the gradient between internal and external temperature is almost doubled when it is compared with the values logged by the T-type thermocouple of the cycler. K-type (Chromel and Alumel) and T-type (Copper-Constantan) thermocouples that are commonly used in cell testing work based on the Seebeck effect that leads to a voltage generated between two dissimilar metals. The Seebeck coefficient of metals changes in a presence of a magnetic field [10] that could be generated by high currents applied during fast charging. The tip of the thermocouple junction is affected in the changing magnetic field resulting in a patristic voltage in the thermocouple output that can lead to large temperature measurement errors in T-type thermocouples [11]. Fig. 5 compares the internal (Int) and

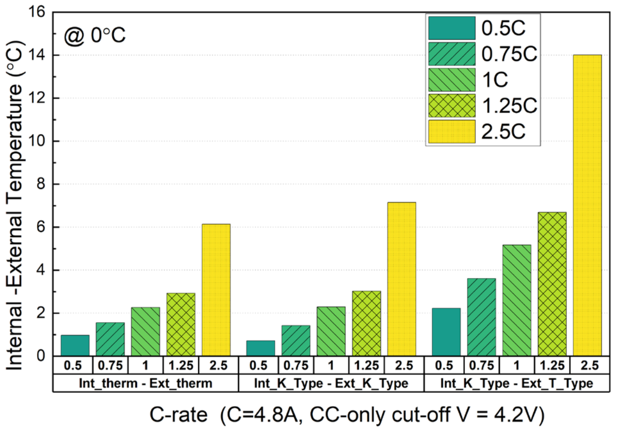

Figure 5 Effect of the type of measurement devices on the gradient of temperature between the internal and external temperatures. To compare the temperature of the same location, thermistor No 4 was chosen. The internal K-type is reported from the internal K-type instrumented cell mounted adjacent to the thermistor instrumented cells.

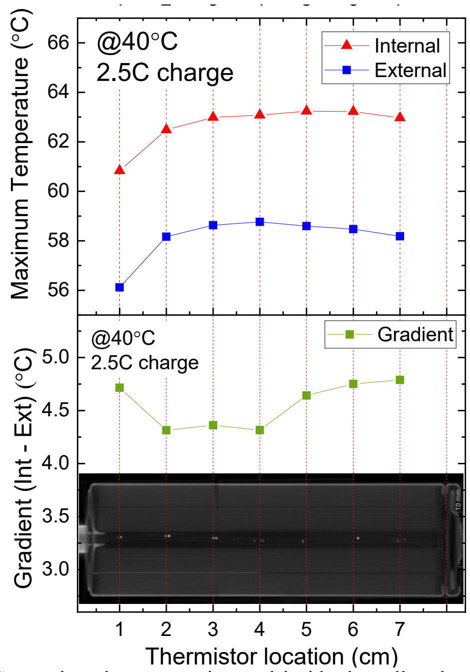

Figure 6 Seven thermistors were inserted inside the cell and a similar array was mounted externally as shown in Fig. 2. The locations of the thermistors are shown on the micro-CT image on the lower figure. The test environment temperature was 40°C and cell was charged up to 4.2V at constant C-rate of 2.5C (12A).

Surface (Ext) temperature measured by thermistors, K-type and T-type thermocouples for a fast-charging cycle performed at environmental temperature of 0°C. It can be observed that the gradient between the internal and external measurement increases with C-rates. K-type error is ~1°C and T-type error is ~8°C when compared with gradient of thermistor No-4.

The thermistor data shown in Fig. 4 is the averaged data from the 7 thermistors for clarity of the figure, that can explain the lower temperatures reported, when it is compared to the values measured by the internal K-type thermocouple located centrally. To further investigate this effect, Fig. 6 matches the maximum temperature recorded from each thermistor array with the micro-CT image of the cell. For both internal and surface arrays of thermistors the thermistor in location 1 (Fig. 2-a) positioned closest to the negative tab logged the lowest temperature. This drop of approximately 2°C can be explained by difficulties mounting array near the edge of the cell, without interfering with the bus-bar connections to the cycler. In the case of the internal thermistor, it can be attributed to better cooling because of the metal fixture that is holding the thermistor array in place. This trend was observed for all cells instrumented with thermistors.

It can be concluded from the above results that single rate fast charging cannot achieve the USABC expectation of fast charging. Not only the required time for FC cannot be achieved using continuous high C-rates, but also it raises safety concerns due to an increased internal temperature of the cell. The other concerns of fast charging at low temperatures (<25°C) and high charge rates (C<1) are Li-plating and consecutive capacity fade. In the next section, these effects will be discussed using a voltage relaxation curve to detect the potential occurrence of Li-plating.

A. Voltage Relaxation Profile and Li-Plating

It was shown in Table 1 that cell resistance was increased, and capacity decreased after the FC cycles above room temperature by 0.3% and 1%, respectively for pristine cells. However, after FC at 10 and 5°C their resistance increased by 1.4% and capacity faded a further 2%. The increase in resistance was 1.7% after the FC at 0°C. It is known that Li-plating causes capacity fade and increases the internal resistance.

The reversible part of plated Li contributes to a distinctive cell voltage relaxation profile (VRP) during the rest period. The differential curves (*dV/dt*) of the OCV immediately after the CC charge allows the reversible plated Li to be estimated. The end of the Li-stripping period is shown by an arrow in Fig. 7. When Li-stripping is continuously occurring, the slope of *dV/dt* curves reach a local minimum because of a nearly flat region in the OCV and then gets to a maximum when the reverse reactions end (Fig. 7-a-1 to -3). Stripping times are reduced when the ambient temperature is increased. The opposite trend can be seen when the charge rate is increased. The time of stripping is lengthened and is the highest for the 1C for all temperatures below 25°C. No Li plating was detected using the VRP method for temperatures of 25 and 40°C for all C-rates (including the 1.25 and 2.5 C cycles). In contrast, even at C-rate as low as 0.5 C there is a change in the *dV/dt* curve for the 10°C test. This is an important observation, considering there is no active cooling in this study and only ambient temperature was monitored. Fig. 4 shows the gradient of internal temperature rise for the cells during 1C charge. The cell temperature rose to 20°C when ambient temperature was 10°C. At temperature below 25°C, the charge transfer rate decreases resulting a more favourable condition for Li-plating as C-rate increases. Therefore, in a real application when active cooling is incorporated, the Li-plating will be exacerbated. In this study the SoC at the end-of-charge was not 100% and yet a considerable amount of reversible plating was detected. The capacity fade shown in Table 1 indicates non reversible plating occurred after only one multi-C-rate cycle (33 hr). Future work will focus on the transferability to different cell formats and chemistries, from cell level to system level, and impact of different sensor technologies and cooling methods

IV. Conclusion

Two types of bespoke internal sensing methods, thermocouple and thermistor sensors developed by [3, 8],

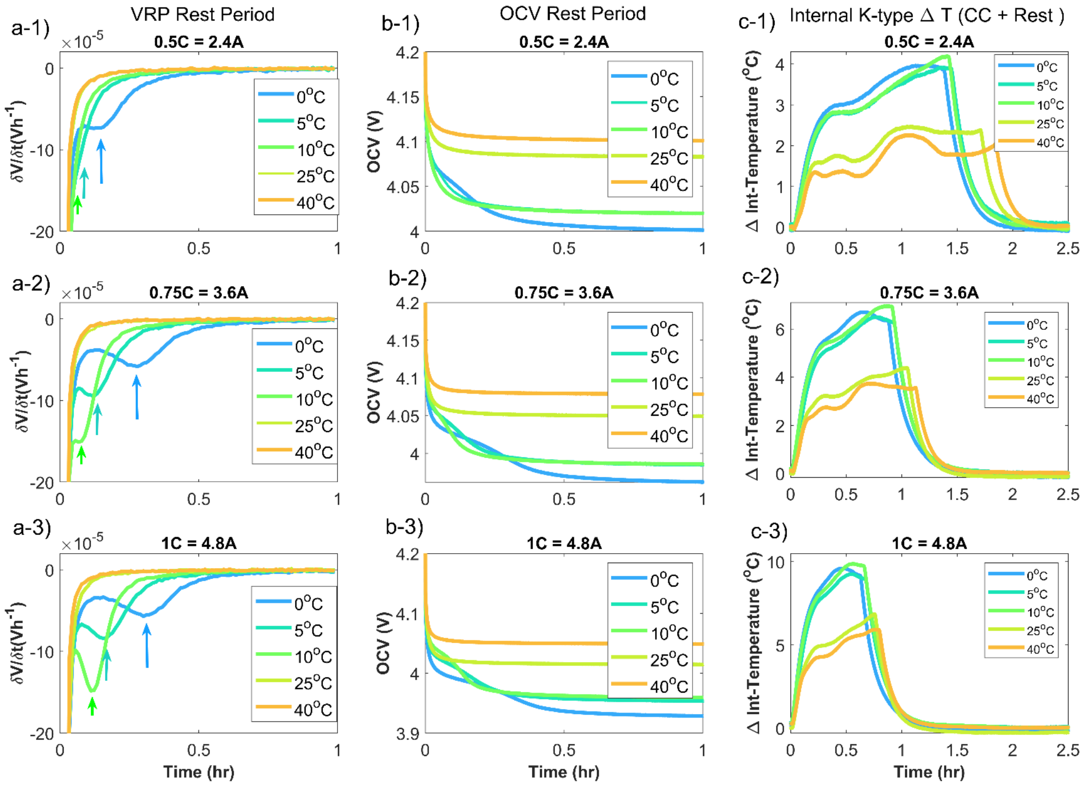

Figure 7 a-1 to a-3 the VRP of the OCV curves on shown in b-1 to b-3. The end of Li-stripping feature is indicated by an arrow for lower temperatures of 0, 5 and 10°C. c-1 to c-3 shows the internal temperature profile during the charge and relaxation period for 0.5C, 0.75C and 1C charge rates.

were used here to show the importance of internal LIB temperature sensing during fast charging.

Here, we demonstrated the significant temperature difference between the internal temperature and external surface temperature monitored by the cell cycler. Internal temperature was always higher than the external regardless of the sensor type. Using traditional surface mount sensors, such as commonly used T-type thermocouples, gave much lower readings when cells were charged using high currents above 1C. A higher temperature gradient was observed using the surface mounting thermistors when compared with the internal thermistors. These findings highlight two main challenges of using external thermocouples as the main safety control during fast charging. Firstly, the most commonly used thermocouples might be affected by the high current passing through the cells due to the magneto-Seebeck effect. Secondly, the internal monitoring of Li-ion batteries produces inherently reliable measurements, the positioning of an external temperature sensor can impact the temperature reading by up to 5°C. Regardless of the temperature rise during charging, we demonstrated the applicability of VRP in detecting Li-plating for all C-rates (as low as 0.5C) for environmental temperature below 25°C. Considering T-type thermocouples are the principal safety control implemented during cell cycling, there is a great potential safety concern when developing new fast charging profiles for high energy density LIB only using traditional surface mounted thermocouples. Therefore, using embedded temperature sensing should be considered when developing new fast charging profiles for EV and aircraft applications.

Acknowledgment

This is research was supported by the Innovate UK Advanced Propulsion Centre Electric BSA (eBSA), Project Number: 75281.

References

[1] P, C.J.: 'Battery Test Manual For Electric Vehicles, Revision 3', in Editor (Ed.)^(Eds.): 'Book Battery Test Manual For Electric Vehicles, Revision 3' (Idaho National Lab, 2015, edn.), pp.

[2] Tomaszewska, A., Chu, Z., Feng, X., O'Kane, S., Liu, X., Chen, J., Ji, C., Endler, E., Li, R., Liu, L., Li, Y., Zheng, S., Vetterlein, S., Gao, M., Du, J., Parkes, M., Ouyang, M., Marinescu, M., Offer, G., and Wu, B.: 'Lithium-ion battery fast charging', eTransportation, 2019, 1, pp. 100011

[3] Gulsoy, B., Vincent, T.A., Sansom, J.E.H., and Marco, J.: 'In-situ temperature monitoring of a lithium-ion battery using an embedded thermocouple for smart battery applications', Journal of Energy Storage, 2022, 54, pp. 105260

[4] Liu, Y.Y., Zhu, Y.Y., and Cui, Y.: 'Challenges and opportunities towards fast-charging battery materials', Nature Energy, 2019, 4, (7), pp. 540-550

[5] Waldmann, T., Hogg, B.-I., and Wohlfahrt-Mehrens, M.: 'Li plating as unwanted side reaction in commercial Li-ion cells – A review', Journal of Power Sources, 2018, 384, pp. 107-124

[6] Campbell, I.D., Marzook, M., Marinescu, M., and Offer, G.J.: 'How Observable Is Lithium Plating?', Journal of The Electrochemical Society, 2019, 166, (4), pp. A725-A739

[7] Konz, Z.M., McShane, E.J., and McCloskey, B.D.: 'Detecting the Onset of Lithium Plating and Monitoring Fast Charging Performance with Voltage Relaxation', ACS Energy Letters, 2020, 5, (6), pp. 1750-1757

[8] Vincent, T.A., Gulsoy, B., Sansom, J.E.H., and Marco, J.: 'In-situ instrumentation of cells and power line communication data acquisition towards smart cell development', Journal of Energy Storage, 2022, 50, pp. 104218

[9] Koleti, U.R., Dinh, T.Q., and Marco, J.: 'A new on-line method for lithium plating detection in lithium-ion batteries', Journal of Power Sources, 2020, 451

[10] Schröder, K., and Otooni, M.: 'Effect of magnetic fields on the absolute Seebeck coefficient and the resistivity of thermocouple wires', Journal of Physics D: Applied Physics, 1971, 4, (10), pp. 1612-1616

[11] Shir, F., Mavriplis, C., and Bennett, L.H.: 'Effect of Magnetic Field Dynamics on the Copper - Constantan Thermocouple Performance', Instrumentation Science & Technology, 2005, 33, (6), pp. 661-671